

UCSF

UC San Francisco Previously Published Works

Title

Type 2 innate lymphoid cells control eosinophil homeostasis.

Permalink

<https://escholarship.org/uc/item/5475r2jz>

Journal

Nature, 502(7470)

ISSN

0028-0836

Authors

Nussbaum, Jesse C
Van Dyken, Steven J
von Moltke, Jakob
et al.

Publication Date

2013-10-01

DOI

10.1038/nature12526

Peer reviewed



Published in final edited form as:

Nature. 2013 October 10; 502(7470): 245–248. doi:10.1038/nature12526.

Type 2 innate lymphoid cells control eosinophil homeostasis

Jesse C. Nussbaum¹, Steven J. Van Dyken¹, Jakob von Moltke¹, Laurence E. Cheng², Alexander Mohapatra³, Ari B. Molofsky⁴, Emily E. Thornton⁵, Matthew F. Krummel⁵, Ajay Chawla^{1,6,7}, Hong-Erh Liang¹, and Richard M. Locksley^{1,3,8}

¹Department of Medicine, University of California San Francisco, San Francisco, CA, USA 94143-0795

²Department of Pediatrics, University of California San Francisco, San Francisco, CA, USA 94143-0795

³Department of Microbiology & Immunology, University of California San Francisco, San Francisco, CA, USA 94143-0795

⁴Department of Laboratory Medicine, University of California San Francisco, San Francisco, CA, USA 94143-0795

⁵Department of Pathology, University of California San Francisco, San Francisco, CA, USA 94143-0795

⁶Department of Physiology, University of California San Francisco, San Francisco, CA, USA 94143-0795

⁷Department of Cardiovascular Research Institute, University of California San Francisco, San Francisco, CA, USA 94143-0795

⁸Department of Howard Hughes Medical Institute, University of California San Francisco, San Francisco, CA, USA 94143-0795

Abstract

Eosinophils are specialized myeloid cells associated with allergy and helminth infections. Blood eosinophils demonstrate circadian cycling, as described over 80 years ago,¹ and are abundant in the healthy gastrointestinal tract. Although a cytokine, interleukin (IL)-5, and chemokines such as eotaxins, mediate eosinophil development and survival,² and tissue recruitment,³ respectively, the processes underlying the basal regulation of these signals remain unknown. Here, we show that serum IL-5 is maintained by long-lived type 2 innate lymphoid cells (ILC2) resident in peripheral tissues. ILC2 secrete IL-5 constitutively and are induced to co-express IL-13 during type 2

Users may view, print, copy, download and text and data- mine the content in such documents, for the purposes of academic research, subject always to the full Conditions of use: http://www.nature.com/authors/editorial_policies/license.html#terms

Correspondence and requests for materials should be addressed to locksley@medicine.ucsf.edu.

Supplementary Information is linked to the online version of the paper at www.nature.com/nature.

Author Contributions J.C.N. performed experiments, interpreted data and wrote the manuscript; L.E.C. provided experimental and imaging assistance; S.V.D., A.M., A.B.M. and J.v.M. provided experimental assistance; E.E.T. performed imaging assays; M.F.K. provided reagents and expertise; H.E.L. generated mouse cytokine reporter strains; A.C. discussed experiments and provided oversight for metabolic studies; R.M.L. directed the studies and wrote the paper with J.C.N.

Author Information The authors declare no competing financial interests.

inflammation, resulting in localized eotaxin production and eosinophil accumulation. In the small intestine where eosinophils and eotaxin are constitutive,⁴ ILC2 co-express IL-5 and IL-13, which is enhanced after caloric intake. The circadian synchronizer vasoactive intestinal peptide (VIP) also stimulates ILC2 through the VPAC2 receptor to release IL-5, linking eosinophil levels with metabolic cycling. Tissue ILC2 regulate basal eosinophilopoiesis and tissue eosinophil accumulation through constitutive and stimulated cytokine expression, and this dissociated regulation can be tuned by nutrient intake and central circadian rhythms.

Eosinophils require survival signals delivered through the common beta-receptor chain (βc) shared by interleukins (IL)-3, IL-5 and granulocyte-macrophage colony stimulating factor (GM-CSF).¹ IL-5 is particularly important, as supported by studies in IL-5⁻⁵ and IL-5 receptor α chain (IL-5R α)-deficient⁶ mice, and in humans using anti-IL-5 and anti-IL-5R α that target eosinophils in disease. Without IL-5 signaling, residual eosinophils have been attributed to IL-3 and GM-CSF, as well as eosinophil chemokines, such as eotaxins, that sequester these cells into tissues.^{1,3}

To identify cells that support eosinophils, we generated IL-5 reporter mice, designated Red5 (recombinase-expressing detector for IL-5; R5).⁷ Cells from these mice contain a tandem dimer red fluorescent protein (tdTomato) linked by an internal ribosomal entry site (IRES) to a Cre element replacing the translation initiation site of the endogenous *Il5* gene, facilitating function-marking, fate-mapping and deletion based on IL-5 expression (Fig. 1a). We validated that the construct disrupts the endogenous *Il5* gene and that R5 fluorescence correlates with IL-5 production using CD4⁺ T cells examined after Th1 or Th2 polarization (Extended Data Fig. 1a-c).

Consistent with prior observations,⁸ CD45⁺R5⁺CD4⁻ cells were present in non-lymphoid tissues, including the brain, heart, lung, kidney, skin, intestine and uterus while few R5⁺ cells were in lymphoid organs, including spleen, bone marrow, lymph nodes or thymus, or in the liver (Fig. 1b and c). In all tissues, the vast majority of R5⁺ cells were small cells (forward-/side-scatter low) that lacked lineage markers for T, B, NK and myeloid cells, and expressed markers for innate lymphoid type 2 cells (ILC2),⁹ including CD90.2 (Thy1), CD127 (IL7R α), KLRG1 and ICOS; T1/ST2 and CD25 expression varied among tissues but were present on all lung R5⁺ ILC2 (Extended Data Fig. 2a). Most (75–80%) CD90.2+T1/ST2⁺ lung ILC2 were R5⁺, and these cells had the highest reporter expression compared to the few ILC2 from bone marrow and lymph nodes (Extended Data Fig. 2b). Sorted R5⁺ ILC2 spontaneously secreted IL-5 in culture, confirming that the reporter marks IL-5 production (Extended Data Fig. 2c). Consistent with prior reports,⁹ numbers of ILC2 and R5⁺ ILC2 were similar in Recombinase Activating Gene (RAG)-deficient mice but were nearly absent in CD127-deficient mice (Extended Data Fig. 3a-c). Correspondingly, serum IL-5 was comparable in wild-type and RAG-deficient mice, reduced to about half-normal levels in heterozygous R5/+ mice, and was not detected in CD127-deficient mice (Fig. 1d).

Few ILC2 were present in lungs of newborns, but within the first week CD90.2+T1/ST2⁺ cells increased, and the percent that were R5⁺ reached adult levels (Fig. 2a, Extended Data Fig. 3d-e). We administered BrdU in drinking water of adult mice for two weeks to label dividing cells and found that fewer than 10% of lung ILC2 were labeled (Extended Data Fig.

3f). Pulse-chase labeling indicated that the decay of labeled ILC2 was substantially slower than CD4⁺ T cells (Fig. 2b). As assessed using multiphoton microscopy, lung R5⁺ ILC2 were embedded in collagen-rich regions near the confluence of medium-sized blood vessels and airways but absent from alveoli (Fig. 2c and data not shown).

Lung eosinophilia is a hallmark of allergic lung disease and helminth migration, but eosinophils are rare in the lung at baseline¹ despite constitutive local IL-5. In prior studies, ILC2 stimulated with cytokines or helminth infection upregulated IL-13,^{10,11} which is genetically linked to IL-5 in mice and humans and induces epithelial eotaxins (including CCL11) and endothelial adhesins necessary for eosinophil trafficking.^{1,3} We crossed R5 mice to Smart13 (S13) reporter mice, in which non-signaling human CD4 marks cells producing IL-13.¹¹ In contrast to resting ILC2, lung ILC2 expressed the IL-13 reporter after infection with the helminth *Nippostrongylus brasiliensis*. All IL-13⁺ ILC2 in the lung were R5⁺, whereas CD4⁺ T cells expressed IL-5, IL-13, or both cytokines, consistent with prior observations (Fig. 3a).¹¹

We crossed R5/R5 mice to mice carrying a ROSA26-flox stop-YFP allele to fate-map cells that expressed the IL-5-linked Cre recombinase and infected the mice with *N. brasiliensis* to elicit a type 2 immune response. After infection, YFP was present only in ILC2 and CD4⁺ T cells, and all YFP⁺ cells were also R5⁺ (Extended Data Fig. 4a-b). We also crossed R5/R5 mice to mice carrying a ROSA26-flox stop-diphtheria toxin A allele to delete IL-5-producing cells. The R5 allele was designed such that expression of the tdTomato reporter precedes Cre-mediated loxP recombination. Therefore, in R5/R5 Deleter mice, a population of R5-lo cells may be detectable before they express the ROSA26-diphtheria toxin. At baseline, R5/R5 and R5/R5 Deleter mice had comparable numbers of total cells and CD4⁺ T cells in the bone marrow, spleen, lung and small intestine lamina propria (Extended Data Fig. 4c), but R5⁺ ILC2 were deleted in the lung (Fig. 3b) and small intestine (Extended Data Fig. 4d).

To study the activity of lung ILC2 in the absence of Th2 cells, we crossed R5/R5 and R5/R5 Deleter mice onto a RAG-deficient background and administered IL-2 and IL-33.^{10,12,13} As expected, cytokine-activated ILC2 in R5/R5 RAG-deficient mice showed increased surface KLRG1 expression and R5 MFI (Extended Data Fig. 5a). Cytokine administration increased the ILC2 population and induced eotaxin-1 (CCL11) in lungs of R5/R5 RAG-deficient mice but not in RAG-deficient R5/R5 Deleter mice (Fig. 3c). ILC2 deficiency was bypassed by administering IL-13, which partially restored eotaxin levels.

Whereas eosinophils are rare in the lung at baseline, they are abundant in other tissues, such as the small intestine lamina propria, where they depend on CCL11,⁴ and are absent in mice that lack ILC2.^{13,14} Our finding that ILC2 in the lung can control eosinophil recruitment through dissociated expression of IL-5 and IL-13 led us to explore the role of ILC2-derived cytokines in the basal regulation of peripheral eosinophils. We measured serum IL-5 at 10:00 and at 22:00 and found that the levels correlated with the circadian variation in blood eosinophils.¹⁵ Although influenced by the adrenal-cortical axis,¹⁵ blood eosinophils can be dominantly synchronized by meal timing.¹⁶ Mice fasted for 16 hours exhibited suppressed serum IL-5 and blood eosinophils at 10:00 (Fig. 4a-b). To minimize effects of altered light-

dark cycle or stress induced by fasting, we restricted two groups of mice to feeding at night only or day only, allowed both groups to acclimate for 9 days, and analyzed them at 8:00 (Extended Data Fig. 6a). Unlike lung ILC2, lamina propria ILC2 express IL-13 constitutively, and this was increased in the morning if mice had just been in a fed as opposed to fasted cycle (Fig. 4c and Extended Data Fig. 6b); the numbers of ILC2 remained constant (Extended Data Fig. 6c). IL-13 reporter expression by intestinal ILC2 at 8:00 was diminished after a 16-hr overnight fast (Extended Data Fig. 6d) and restored by administering an evening food (but not water) gavage at 22:00 (Fig. 4d).

The response of small intestine ILC2 to caloric input raised the possibility that these cells could respond to hormonal cues induced by feeding. Indeed, purified intestinal ILC2, most of which were R5+ (Extended Data Fig. 7a), released detectable IL-5 when incubated with IL-7 alone, but increased IL-5 production with addition of vasoactive intestinal peptide (VIP) but not ghrelin or enterostatin (Fig. 4e and Extended Data Fig. 7b). The effect on lung ILC2 was similar (Extended Data Fig. 7c). VIP is a member of the secretin family of neuropeptides, which are expressed throughout the nervous system. They are highly expressed in intestinal neurons, coordinating pancreatic secretion with smooth muscle relaxation in response to feeding,¹⁷ and in neurons of the suprachiasmatic nucleus (SCN), relaying environmental cues necessary to synchronize central circadian oscillators.¹⁸ VPAC2-deficient and VIP-deficient mice exhibit similar defects in circadian behavior,^{19,20} and rhythms mediated by VPAC2 are entrained by feeding.²¹

We hypothesized that VIP might signal through VPAC2 on ILC2. VIP and its receptors are also expressed by immune cells, and signals through VPAC2 have been implicated in Th2 cell expansion, survival and cytokine production.²² Mice deficient in VPAC2 trend toward decreased circulating eosinophils at rest and delayed infiltrating eosinophils with allergic challenge.²³ We detected both VIP receptor type 1 (VPAC1) and type 2 (VPAC2) mRNA in intestinal and lung ILC2, whereas VPAC2 expression was undetectable in eosinophils and low in macrophages and CD4+ T cells (Fig. 4f). Comparable levels of IL-5 were induced in culture with VIP or with a VPAC2-specific agonist (Fig. 4e and Extended Data Fig. 7c).²⁴ VPAC2 is a G protein-coupled receptor that can associate with G α_s to activate adenylate cyclase.²⁵ Consistent with this, we also induced comparable IL-5 levels bypassing the receptor with dibutyryl-cAMP (Fig. 4e).

First noted in humans over 80 years ago,²⁶ circadian variation of blood eosinophils has been linked to neuroendocrine¹⁵ and metabolic¹⁶ cycling. As shown here, long-lived ILC2 in peripheral tissues are the predominant source of circulating IL-5, and their close association with vasculature positions these cells for eosinophil recruitment. After stimulation by epithelial and/or Th2 cytokines, lung ILC2 increase IL-5 and co-express IL-13, leading to local eosinophil accumulation, a process that mimics the post-prandial response of intestinal ILC2 to caloric intake. Further, ILC2 express functional VPAC2 receptors, providing a potential mechanism linking these dispersed tissue resident cells with central circadian and metabolic rhythms. Intestinal eosinophils are normal in germ-free animals,⁴ and IL-13+ ILC2 are found in human fetal gut,²⁷ suggesting that these biologic pathways are independent of intestinal microbiota. Although further study is needed, our findings suggest that eosinophils are linked to basal circadian oscillations through ILC2 activation and raise

the possibility that helminthic parasites may have co-opted these fundamental pathways of host metabolic homeostasis.

METHODS (ONLINE ONLY)

IL-5 reporter mice

R5 IL-5 reporter mice were generated by homologous gene targeting in C57BL/6 embryonic stem cells. The previously published plasmid pKO915-DT (Lexicon) containing the Basoph8 reporter¹⁷ was modified to express tdTomato in place of YFP, such that the cassette now contained (in order from 5' to 3') genomic sequence of the rabbit β -globin gene partial exon 2–3, the gene encoding tdTomato (Clontech), encephalomyocarditis virus IRES, humanized Cre recombinase, bovine growth hormone poly(a), and a *loxP*-flanked neomycin resistance cassette. Homologous arms straddling the *Il5* translation initiation site (3.8 kb toward 5', containing the promoter and 5' UTR and 3.0 kb toward 3', containing the start ATG halfway through exon 3) were amplified from C57BL/6 genomic DNA using Phusion polymerase (Finnzymes) and cloned into the cassette by standard methods. The construct was linearized with NotI and transfected by electroporation into C57BL/6 embryonic stem cells. Cells were grown on irradiated feeders with the aminoglycoside G418 in the media, and neomycin-resistant clones were screened for 5' and 3' homologous recombination by PCR. Eleven positive clones were subsequently tested (and all eleven confirmed) by 5' and 3' Southern Blot. Two clones were selected for injection into albino C57BL/6 blastocysts to generate chimeras, and the male pups with highest ratios of black-to-white coat color from a single clone were selected to breed with homozygous CMV-Cre transgenic C57BL/6 females (B6.C-Tg(CMV-cre)1Cgn/J; 006054, obtained from The Jackson Laboratory) to excise the neomycin resistance cassette. The CMV-Cre transgene is X-linked and the males from this cross were bred to wild-type C57BL/6 females to remove the CMV-Cre allele. Male and female R5/+ offspring were intercrossed to yield R5/R5 homozygotes.

Mice

β -actin-cyan fluorescent protein mice (B6.129(ICR)-Tg(CAG-ECFP)CK6Nagy/J; 004218), *Rag1*^{−/−} mice (B6.129S7-*Rag1*^{tm1Mom}/J; 002216), *Il7ra*^{−/−} mice (B6.129S7-*Il7*^{tm1Imx}/J; 002295), and ROSA-YFP mice (B6.129X1-*Gt(ROSA)26Sor*^{tm1(EYFP)Cos}/J; 006148) were from The Jackson Laboratory. ROSA-DTA and Smart13 mice have been described.¹¹ *Rag1*^{−/−} mice were maintained on SCIDS MD's "Breeders Formula" antibiotic tablets (Bio-Serv). Mice were fed ad lib except when feeding was restricted to 12 hours daily (7:00 to 19:00 or vice versa) or during 16-hour fasting. For gavage experiments, mice previously fed standard chow ad lib were fasted at 16:00 before receiving water or a 1:1 mixture of high-fat chow (Research Diets) and 20% dextrose by oral gavage, representing 13% of ad lib caloric intake at 22:00. Mice used in experiments were mixed gender, between 6 and 10 weeks old, on the C57BL/6 background and were maintained according to institutional guidelines in specific pathogen-free facilities at the University of California, San Francisco (San Francisco, CA).

Lung imaging

Lung slices were prepared using a modification of established methods.²⁹ After euthanasia, lungs were inflated with 1 ml of 2% low-melt agarose (Type VII, Sigma-Aldrich), excised and placed in 5 ml cold PBS, and 600 μ m sections were cut on a vibratome (Model G, Oxford Laboratories). Lung sections were maintained in PBS at room temperature until mounting. All sections were mounted with PBS and imaged on a multiphoton microscope with data collected in three channels (CFP, GFP, RFP). Images were analyzed with Imaris software (Bitplane). Software spot detection algorithms were used to identify cells.

Nippostrongylus brasiliensis infection and cytokine administration

Mice were infected with 500 *N. brasiliensis* third-stage larvae (L3) and were killed at the indicated timepoints for analysis of the mediastinal and mesenteric lymph nodes, lungs, and bone marrow. Procedures for maintaining as described.¹¹ Rag1^{-/-} mice were given IL-2, IL-33, and IL-13 as follows: IL-2 complexes were generated by incubating 0.5 μ g mouse IL-2 (R&D Systems) with 5 μ g anti-IL2 (JES6-A12, R&D Systems), and then administered intraperitoneally in 200 μ l PBS on day 0; IL-33 was given in two daily doses of 500 ng in 30 μ l PBS intranasally on days 0 and 1; some animals additionally received 1 μ g of IL-13 intranasally with the daily doses of IL-33 on days 0 and 1. On day 2, the lungs were harvested. The left lobe was treated as above and cells were isolated for flow cytometry. The right lung was homogenized in 1 ml of PBS using GentleMACS C tubes (Miltenyi Biotec), pelleted, and the supernatant was filtered through a 0.8 μ m strainer and used for CCL11 ELISA (R&D Systems).

In vitro CD4⁺ T cell polarization

CD4⁺ T cells were isolated from the lymph nodes of R5/R5, R5/+ and wild-type C57BL/6 mice using negative selection MACS beads (Miltenyi Biotec) and cultured in plates pre-coated with anti-CD3 ϵ and anti-CD28 (BD Pharmingen) under standard Th2 polarization conditions for four days, as described¹¹. On day 4 the cells were washed and re-plated with 50 U/ml recombinant human IL-2 (R&D Systems) and then split at day 6 and day 8. On day 9 or 10, the cells were plated at 2×10^6 /ml in plates pre-coated with anti-CD3 ϵ . One well was used for intracellular cytokine staining: 3 μ M monensin was added at 18 hours, and at 24 hours the cells were stained with phycoerythrin-cyanine 7 (PE-Cy7) anti-CD3 (17A2, eBioscience) and peridinin chlorophyll protein-cyanine 5.5 (PerCP-Cy5.5) anti-CD4 (RM4-5, eBiosciences) and with Violet LIVE/DEAD (Invitrogen) prior to fixation in 2% paraformaldehyde (PFA, Electron Microscopy Sciences) in PBS, permeabilization with 0.5% saponin/3% fetal calf serum (FCS) in PBS, and staining with allophycocyanin (APC) anti-IL-5 (TRFK5, BD Pharmingen), fluorescein (FITC) anti-IFN- γ (XMG1.2, BD Pharmingen), eFluor 660 anti-IL-13 (50-7133-80, eBioscience), or PE anti-IL-4 (11B11, BD Pharmingen). For the remaining wells, restimulation on anti-CD3 ϵ was continued for 4 days and each day supernatant was collected and stored at -20° C, and one well was harvested for flow cytometry.

Cell preparation from tissues

We performed transcardiac perfusion with 20 ml of PBS prior to harvesting organs. Single-cell suspensions were prepared as follows: spleen, lymph nodes and thymus were mechanically dissociated through 70 μ m filters and bone marrow was processed by crushing a single femur with a mortar and pestle prior to 70- μ m filtration. Whole lungs, heart, kidney and uterus were minced, digested by gentle shaking in 5 ml HBSS with 0.1 WU/ml Liberase TM (Roche) and 25 μ g/ml DNase I (Roche) for 30 minutes at 37° C, and then mechanically dissociated using GentleMACS C tubes (Miltenyi Biotec) followed by a 70- μ m filter. Brain and skeletal muscle were similarly digested in Liberase/DNase, but were resuspended in 40% Percoll (GE Healthcare), underlaid with 90% Percoll and centrifuged at 2200 rpm for 20 minutes at 20° C to isolate the hematopoietic cells from the interphase. Liver was minced, passed through a 70 μ m filter and separated using a 90/40 Percoll gradient without enzymatic digestion. Skin and small intestinal lamina propria were prepared as described.²⁸ Peyer's patches were treated like lymph nodes (see above). Cells from all tissues were washed with PBS containing 3% (v/v) FCS and 1 mg/L sodium azide.

Flow cytometry

The single-cell suspensions prepared above were pelleted and incubated with anti-CD16/CD32 monoclonal antibodies (UCSF Antibody Core Facility) for 10 minutes at 4° C. The cells were stained with antibodies to surface markers for 25 minutes at 4° C and, if necessary, were washed and incubated with secondary antibodies for an additional 25 minutes at 4° C. After a final wash, cells were resuspended in 1 μ g/ml 4',6-diamidino-2-phenylindole (DAPI, Roche) for dead cell exclusion. Monoclonal antibodies from Biolegend included: Pacific Blue (PB) anti-Ly-6G/Ly-6C (Gr-1), PB anti-CD3 (17A2), PB anti-CD8 α (53-6.7), PB anti-CD11b (M1/70), PB anti-CD11c (N418), PB anti-NK1.1 (PK136), Alexa Fluor 488 anti-CD3 (17A2); FITC anti-Fc ϵ RI α (MAR-1); PerCP-Cy5.5 anti-CD11c (N418), and anti-Gr-1 (RB6-8C5); Brilliant Violet (BV) 605 anti-CD4 (RM4-5) and anti-CD11b (M1/70); BV 711 anti-CD4 (RM4-5); Alexa Fluor 647 anti-Fc ϵ RI α (MAR-1); APC anti-KLRG1 (2F1), anti-ICOS (C398.4A), and anti-CD45R/B220 (RA3-6B2); APC-Cy7 anti-CD25 (PC-61) and anti-CD45 (30-F11); and biotinylated anti-ICOS (C398.4A). Monoclonal antibodies from eBioscience included: Alexa Fluor 647 anti-CD19 (eBio1D3); APC anti-NK1.1 (PK136); PE-Cy7 anti-CD5 (53-7.3); APC-eFluor 780 anti-CD11b (M1/70) and anti-CD90.2 (53-2.1); PerCP-eFluor 710 anti-KLRG1 (2F1); PerCP-Cy5.5 anti-CD127 (A7R34); APC anti-human CD4 (RPA-T4) was used to detect human CD4 expressed in Smart13 mice. Monoclonal antibodies from BD Biosciences included: FITC anti-TCR β (H57-597); PerCP-Cy5.5 anti-CD11b (M1/70), anti-CD19 (1D3), and anti-CD8 α (53-6.7); Alexa Fluor 647 anti-SiglecF (E50-2440); APC anti-CD11c (HL3); APC-Cy7 anti-Gr-1 (RB6-8C5); PE-Cy7 anti-CD11c (HL3) and anti-NK1.1 (PK136); Horizon V500 anti-CD4 (RM4-5) and anti-CD45 (30-F11); and biotinylated anti-KLRG1 (2F1). Monoclonal antibodies from Invitrogen included APC anti-Gr-1 (RB6-8C5) and APC Alexa Fluor 750 anti-CD45R/B220 (RA3-6B2). FITC and biotinylated anti-T1/ST2 (DJ8) were from MD Bioproducts. An Alexa Fluor 488-conjugated anti-SiglecF antibody was generated using purified anti-SiglecF (E50-2440, BD Pharmingen) with an Alexa Fluor 488 Monoclonal Antibody Labeling Kit (Invitrogen). Secondary antibodies included streptavidin (SA) V500 (BD Horizon), SA BV 605 and BV 650 (Biolegend). Cell counts were performed using CountBright beads

(Invitrogen). Samples were analyzed on an LSR II (BD Biosciences) with four lasers (403 nm, 488 nm, 535 nm, and 633 nm) and data was analyzed with FlowJo software (Treestar).

5-Bromo-2'-deoxyuridine (BrdU)

Naïve mice received 300 µg BrdU (Sigma-Aldrich) in 300 µl PBS as an intraperitoneal injection on the day that their standard drinking water was exchanged for water containing 800 µg/ml BrdU and 220 µg/ml sodium saccharin (Sigma-Aldrich). The water bottles were covered in aluminum foil and water was changed every 3 days. On the indicated days, lungs and thymus were harvested. Single-cell suspensions were prepared as above and cells were stained with antibodies for surface markers followed by violet fixable LIVE/DEAD (Invitrogen). Cells were then fixed in 4% PFA in PBS at room temperature for 15 minutes, followed by staining for BrdU incorporation using the APC BrdU Flow Kit (BD Biosciences).

ILC2 culture

ILC2 from lungs and small intestines of mice were sorted on a MoFlo XDP gating on cells negative for lineage markers (CD3, CD4, CD5, CD8, CD19, CD11b, CD11c, Gr-1, NK1.1), followed by CD90.2+R5+ selection (lung) or Lin-KLRG1+R5+ selection (intestine). In some experiments, wild-type organs were prepared and gated on cells negative for lineage markers (as above), followed by CD90.2+CD25+ selection (lung) or CD45+KLRG1+ selection (intestine). For Elispot, cells were cultured at 3000 per well in 10 ng/ml IL-7 for 48 hours. For supernatant IL-5, cells were cultured at 5000 per well for 18 hours, or at 10,000 per well for 6 hours, in 10 ng/ml IL-7 plus 1 µM VIP, VPAC2-specific agonist (BAY 55-9837), ghrelin, or enterostatin or 100 µM dibutyryl cAMP.

IL-5 detection

Supernatant from T cell cultures was assayed for IL-5 by ELISA, performed in duplicate serial 2-fold dilutions using IL-5 DuoSet (R&D Systems). For Elispot, ILC2 were plated at 3000 per well in a 96-well Multiscreen filter plate (Millipore) pre-coated with anti-IL-5 capture antibody (eBioscience). The cells were cultured in complete RPMI-10% FCS and after 48 hours the wells were washed and treated according to manufacturer's ELISPOT protocol (eBioscience). IL-5 from serum and ILC2 culture supernatant was measured using an Enhanced Sensitivity Flex Set with Enhanced Sensitivity Cytometric Bead Array kit (BD). Bead fluorescence was captured on an LSRII (BD) and analyzed using Flow Cytometric Analysis Program (FCAP) Array software (BD).

Quantitative RT-PCR

ILC2 (see above), lung macrophages (CD11b+CD11c+), blood eosinophils (SiglecF+CD11b+SSC-hi), and blood and intestinal CD4+ cells were sorted on a MoFlo XDP and RNA was isolated using the Micro RNeasy kit (Qiagen). The RNA was reverse transcribed with SuperScript III (Invitrogen), and the resulting cDNA was used as template for quantitative PCR with the Power SYBR Green kit on a StepOnePlus cycler (Applied Biosystems). Intron-spanning *Vpac1* and *Vpac2* primers were as described.³⁰ Transcripts were normalized

to 40S ribosomal protein S17 (*Rps17*) (sense: CGCCATTATCCCCAGCAAG; antisense: TGTCGGGATCCACCTCAATG).

Experimental design and statistics

All experiments comparing treatment groups were made using randomly assigned littermates without investigator blinding. Comparisons among mice of different litters were made using age- and gender-matched cohorts. Cohort sizes were chosen after estimating effect size and consulting power tables, and data were analyzed for statistical significance after at least two repeated experiments. Results from independent experiments performed similarly were pooled. All data points reflect biological replicates; technical replicates were averaged to yield a single value for analysis. No data were excluded. All data were analyzed using Prism (GraphPad Software): to compare means in BrdU experiments and ILC2 culture supernatants we used paired two-tailed Student's *t* tests and significance was defined as $p < 0.05$. Comparison across multiple groups in (Extended Data Fig. 3c) was performed using Kruskal-Wallis. Otherwise, all data were analyzed by comparison of means using unpaired two-tailed Student's *t* tests. If the groups to be compared had significantly different variances ($p < 0.05$ by *F* test) then Welch's post-test was performed. Figures display means \pm standard error of the mean (SEM) unless otherwise noted.

Supplementary Material

Refer to Web version on PubMed Central for supplementary material.

Acknowledgements

We thank the NIH Tetramer Core Facility for reagents, B. Sullivan, N. Flores, M. Consengco, and Z. Wang for technical expertise, and M. Anderson, C. Lowell and M. McCune for comments on the manuscript. Supported by NIH (AI026918, AI030663, AI078869, HL107202), the Diabetes Endocrinology Research Center grant (DK063720), the Howard Hughes Medical Institute and the Sandler Asthma Basic Research Center at the University of California San Francisco. J.C.N. supported by NIH Training Grants (AI007641 and AI007334).

REFERENCES

1. Rothenberg ME, Hogan SP. The Eosinophil. *Annual Review of Immunology*. 2006; 24:147–174.
2. Takatsu K, Nakajima H. IL-5 and eosinophilia. *Curr Opin Immunol*. 2008; 20:288–294. [PubMed: 18511250]
3. Pope S, et al. IL-13 induces eosinophil recruitment into the lung by an IL-5 and eotaxin-dependent mechanism. *J Allergy Clin Immunol*. 2001; 108:594–601. [PubMed: 11590387]
4. Mishra A, Hogan S, Lee J, Foster P, Rothenberg M. Fundamental signals that regulate eosinophil homing to the gastrointestinal tract. *J Clin Invest*. 1999; 103:1719–1727. [PubMed: 10377178]
5. Kopf M, et al. IL-5-deficient mice have a developmental defect in CD5+ B-1 cells and lack eosinophilia but have normal antibody and cytotoxic T cell responses. *Immunity*. 1996; 4:15–24. [PubMed: 8574848]
6. Yoshida T, et al. Defective B-1 cell development and impaired immunity against *Angiostrongylus cantonensis* in IL-5R alpha-deficient mice. *Immunity*. 1996; 4:483–494. [PubMed: 8630733]
7. Molofsky AB, et al. Innate lymphoid type 2 cells sustain visceral adipose tissue eosinophils and alternatively activated macrophages. *J Exp Med*. 2013; 210:535–549. [PubMed: 23420878]
8. Ikutani M, et al. Identification of innate IL-5-producing cells and their role in lung eosinophil regulation and antitumor immunity. *J Immunol*. 2012; 188:703–713. [PubMed: 22174445]

9. Spits H, Cupedo T. Innate lymphoid cells: emerging insights in development, lineage relationships, and function. *Annu Rev Immunol.* 2012; 30:647–675. [PubMed: 22224763]
10. Price A, et al. Systemically dispersed innate IL-13-expressing cells in type 2 immunity. *Proc Natl Acad Sci U S A.* 2010; 107:11489–11494. [PubMed: 20534524]
11. Liang HE, et al. Divergent expression patterns of IL-4 and IL-13 define unique functions in allergic immunity. *Nat Immunol.* 2012; 13:58–66. [PubMed: 22138715]
12. Neill DR, et al. Nuocytes represent a new innate effector leukocyte that mediates type-2 immunity. *Nature.* 2010; 464:1367–1370. [PubMed: 20200518]
13. Moro K, et al. Innate production of TH2 cytokines by adipose tissue-associated c-Kit+Sca-1+ lymphoid cells. *Nature.* 2010; 463:540–544. [PubMed: 20023630]
14. Carlens J, et al. Common gamma-chain-dependent signals confer selective survival of eosinophils in the murine small intestine. *J Immunol.* 2009; 183:5600–5607. [PubMed: 19843944]
15. Halberg F, Visscher M, Bittner J. Eosinophil rhythm in mice: range of occurrence; effects of illumination, feeding, and adrenalectomy. *Am J Physiol.* 1953; 174:109–122. [PubMed: 13065505]
16. Pauly J, et al. Meal timing dominates the lighting regimen as a synchronizer of the eosinophil rhythm in mice. *Acta Anat (Basel).* 1975; 93:60–68. [PubMed: 1189901]
17. Lelievre V, et al. Gastrointestinal dysfunction in mice with a targeted mutation in the gene encoding vasoactive intestinal polypeptide: a model for the study of intestinal ileus and Hirschsprung's disease. *Peptides.* 2007; 28:1688–1699. [PubMed: 17606312]
18. Maywood ES, et al. Analysis of core circadian feedback loop in suprachiasmatic nucleus of mCry1-luc transgenic reporter mouse. *Proc Natl Acad Sci U S A.* 2013; 110:9547–9552. [PubMed: 23690615]
19. Harmar AJ, et al. The VPAC(2) receptor is essential for circadian function in the mouse suprachiasmatic nuclei. *Cell.* 2002; 109:497–508. [PubMed: 12086606]
20. Colwell CS, et al. Disrupted circadian rhythms in VIP- and PHI-deficient mice. *Am J Physiol Regul Integr Comp Physiol.* 2003; 285:R939–R849. [PubMed: 12855416]
21. Sheward WJ, et al. Entrainment to feeding but not to light: circadian phenotype of VPAC2 receptor-null mice. *J Neurosci.* 2007; 27:4351–4358. [PubMed: 17442819]
22. Voice J, et al. c-Maf and JunB mediation of Th2 differentiation induced by the type 2 G protein-coupled receptor (VPAC2) for vasoactive intestinal peptide. *J Immunol.* 2004; 172:7289–7296. [PubMed: 15187104]
23. Samarasinghe AE, Hoselton SA, Schuh JM. The absence of VPAC2 leads to aberrant antibody production in *Aspergillus fumigatus* sensitized and challenged mice. *Peptides.* 2011; 32:131–137. [PubMed: 20923692]
24. Tsutsumi M, et al. A potent and highly selective VPAC2 agonist enhances glucose-induced insulin release and glucose disposal: a potential therapy for type 2 diabetes. *Diabetes.* 2002; 51:1453–1460. [PubMed: 11978642]
25. Dickson L, Finlayson K. VPAC and PAC receptors: From ligands to function. *Pharmacol Ther.* 2009; 121:294–316. [PubMed: 19109992]
26. Domarus, Av. Die bedeutung der kammerzählung der eosinophilen für die klinik. *Deutsch Arch Klin Med.* 1931; 171:333–358.
27. Mjösberg JM, et al. Human IL-25- and IL-33-responsive type 2 innate lymphoid cells are defined by expression of CCR4 and CD161. *Nat Immunol.* 2011; 12:1055–1062. [PubMed: 21909091]
28. Sullivan BM, et al. Genetic analysis of basophil function in vivo. *Nat Immunol.* 2011; 12:527–535. [PubMed: 21552267]
29. Thornton EE, et al. Spatiotemporally separated antigen uptake by alveolar dendritic cells and airway presentation to T cells in the lung. *J Exp Med.* 2012; 209:1183–1199. [PubMed: 22585735]
30. Vomhof-DeKrey EE, et al. Radical reversal of vasoactive intestinal peptide (VIP) receptors during early lymphopoiesis. *Peptides.* 2011; 32:2058–2066. [PubMed: 21878358]

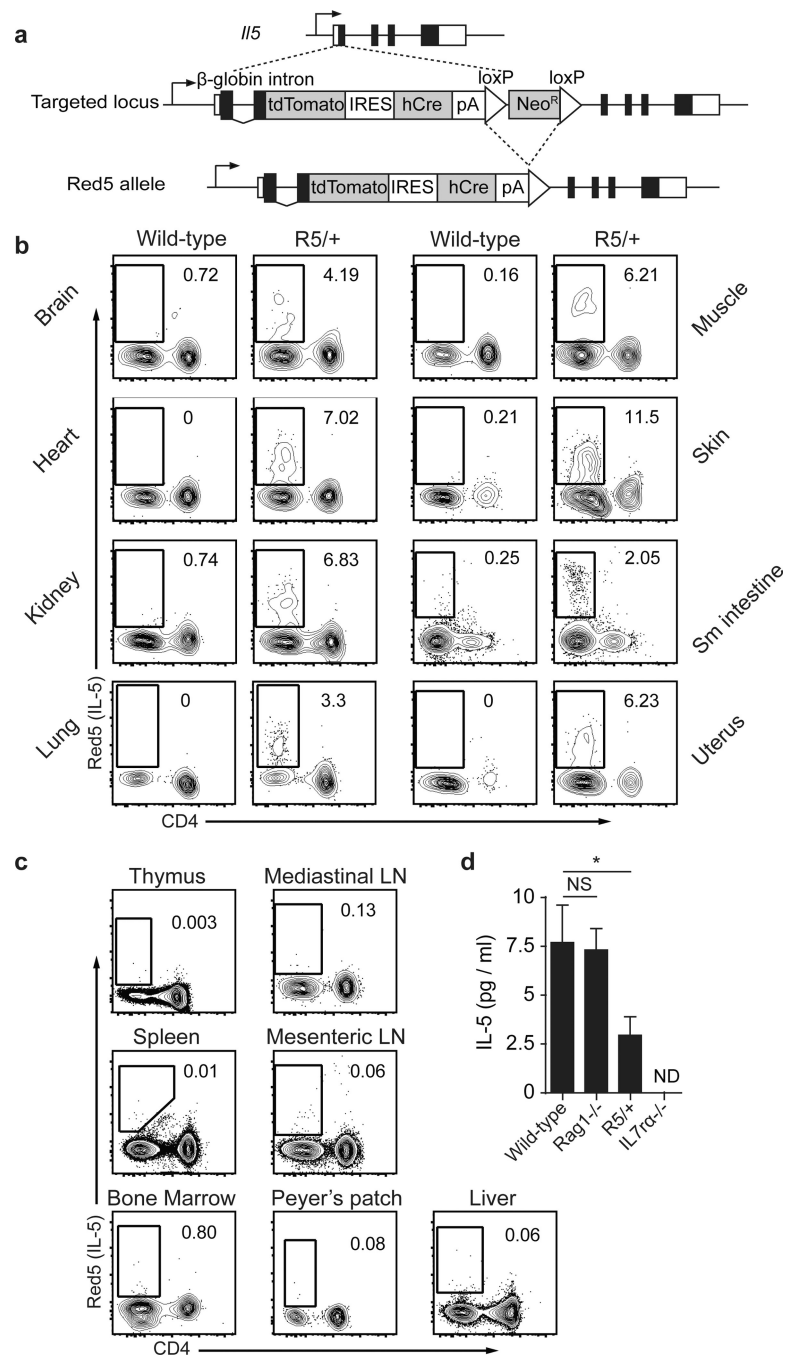


Figure 1. Innate cells produce IL-5 in tissues at rest

a, Schematic of targeting construct. **b-c**, Flow cytometry of tissues, previously gated on CD45+CD90.2+ cells in wild-type and R5/+ (**b**) or CD90.2+ cells in R5/R5 (**c**) naïve mice. **d**, Serum IL-5. Data representative of two independent experiments with two mice per group (**b-d**) or pooled from three independent experiments for 7 (wild-type), 4 (Red5), or 8 (others) mice per group (**c**). LN, lymph nodes; ND, none detected; NS not significant; *, $p < 0.05$.

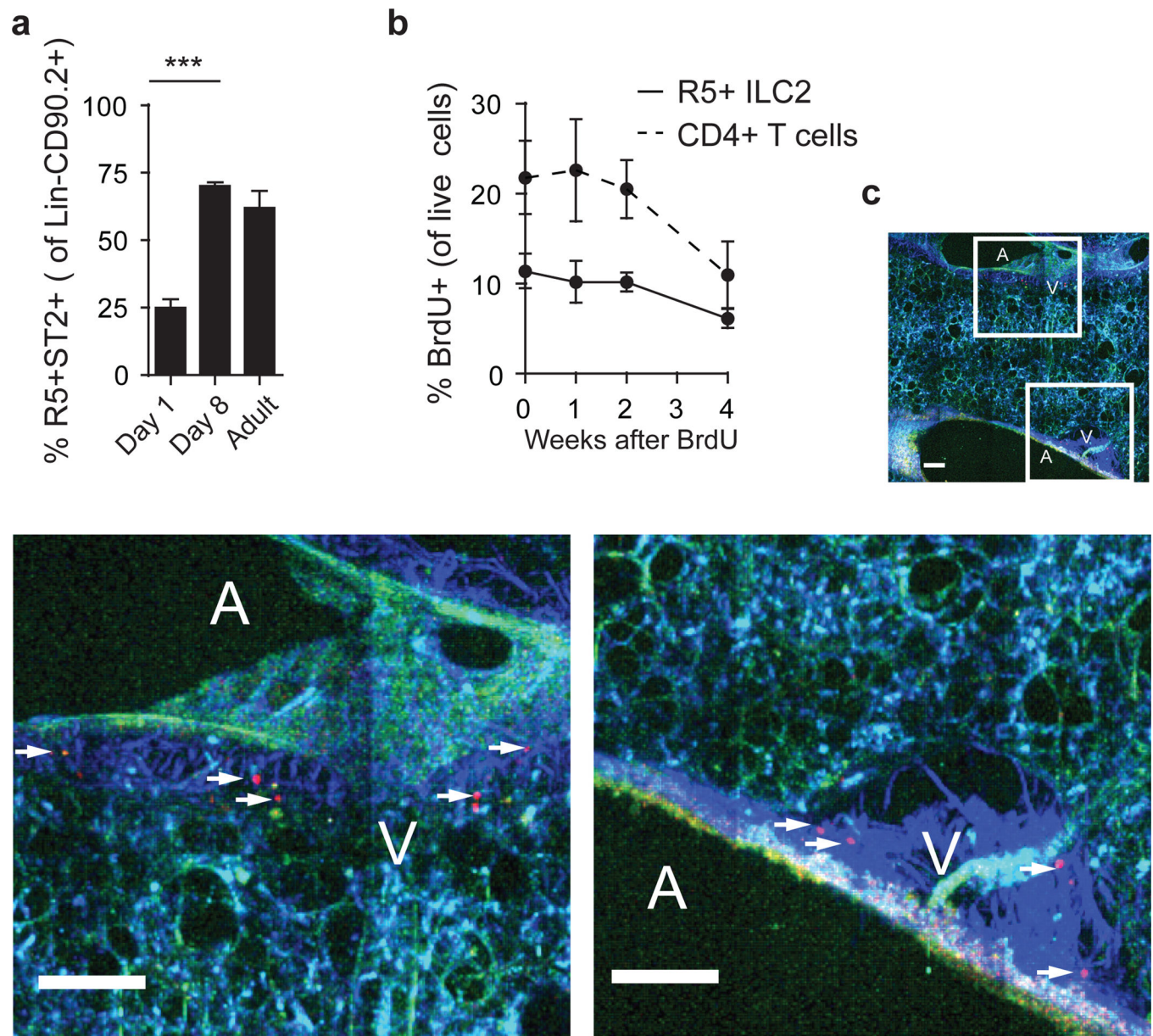


Figure 2. ILC2 expand after birth and persist in collagen-rich structures

a, Percent of lung Lin-CD90.2+ cells R5+T1/ST2 on day 1, day 8, or week 8. **b**, Percent BrdU+ of R5+ ILC2 and total CD4+ cells in lung after four weeks BrdU. **c**, Representative multiphoton images of tdTomato fluorescence (red) in naïve R5/R5 actin-CFP mice; CFP and autofluorescence in blue and green, respectively. A=airway. V=vasculature. Collagen second harmonic appears blue. Scale bars 100 μ m. Data pooled from three independent experiments for 5 (Day 1), 6 (Day 8), or 4 (Adult) mice per group (**a**); or pooled from two independent experiments for 5 (week 0), 6 (week 1), or 3 (others) mice per group (**b**), represented as mean \pm SEM. Images represent 8 regions taken from two mice. Lin, Lineage markers (B220, CD5, CD11b, CD11c, Ly6G, Fc ϵ RI, and NK1.1); ***, $p < 0.01$ by Student's t test.

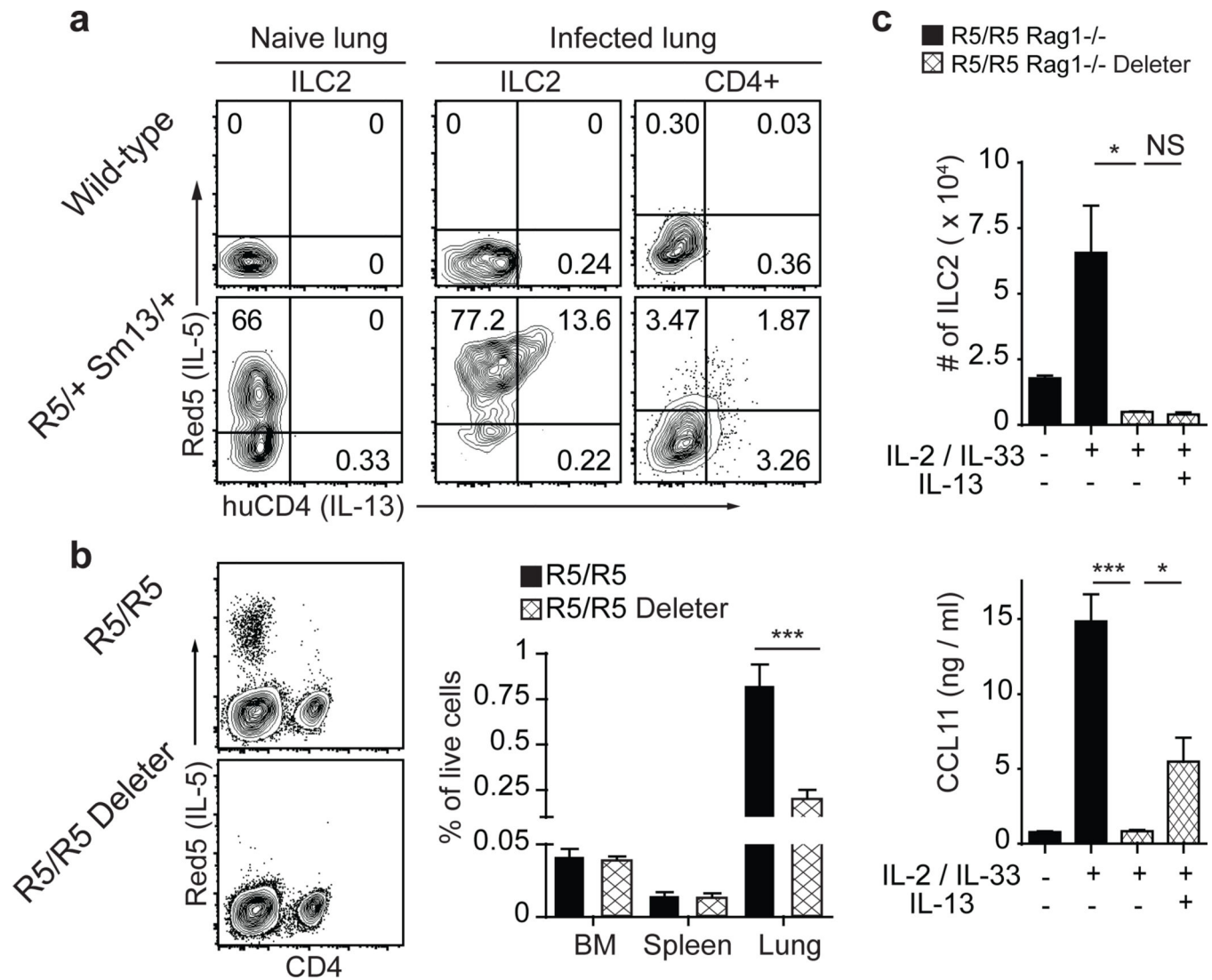


Figure 3. IL-5 and IL-13 co-expression in lung ILC2

a, Lung IL-5 and IL-13 reporter expression before and after infection. **b**, Flow cytometry of CD90.2+ lung cells and percent with ILC2 surface markers (CD90.2 and either KLRG1, T1/ST2 or CD25) at rest. **c**, ILC2 (left lung) and CCL11 concentration (right lung) after IL-2, IL-33, and IL-13 treatment. Data representative of three independent experiments with 4 (naïve R5+S13+), 5 (infected R5+S13+), or 2 (others) mice per group (**a**), pooled from three independent experiments for 6 (R5/R5 bone marrow and spleen) or 9 (all others) mice per group (**b**), or pooled from two independent experiments for 8 (R5/R5 + IL-2/IL-33), 5 (R5/R5 Deleter + IL-2/IL-33/IL-13), or 3 (others) mice per group (**c**). Represented as mean \pm SEM. huCD4, human CD4; BM, bone marrow; NS, not significant; *, $p < 0.05$; ***, $p < 0.001$ by Student's *t* test.

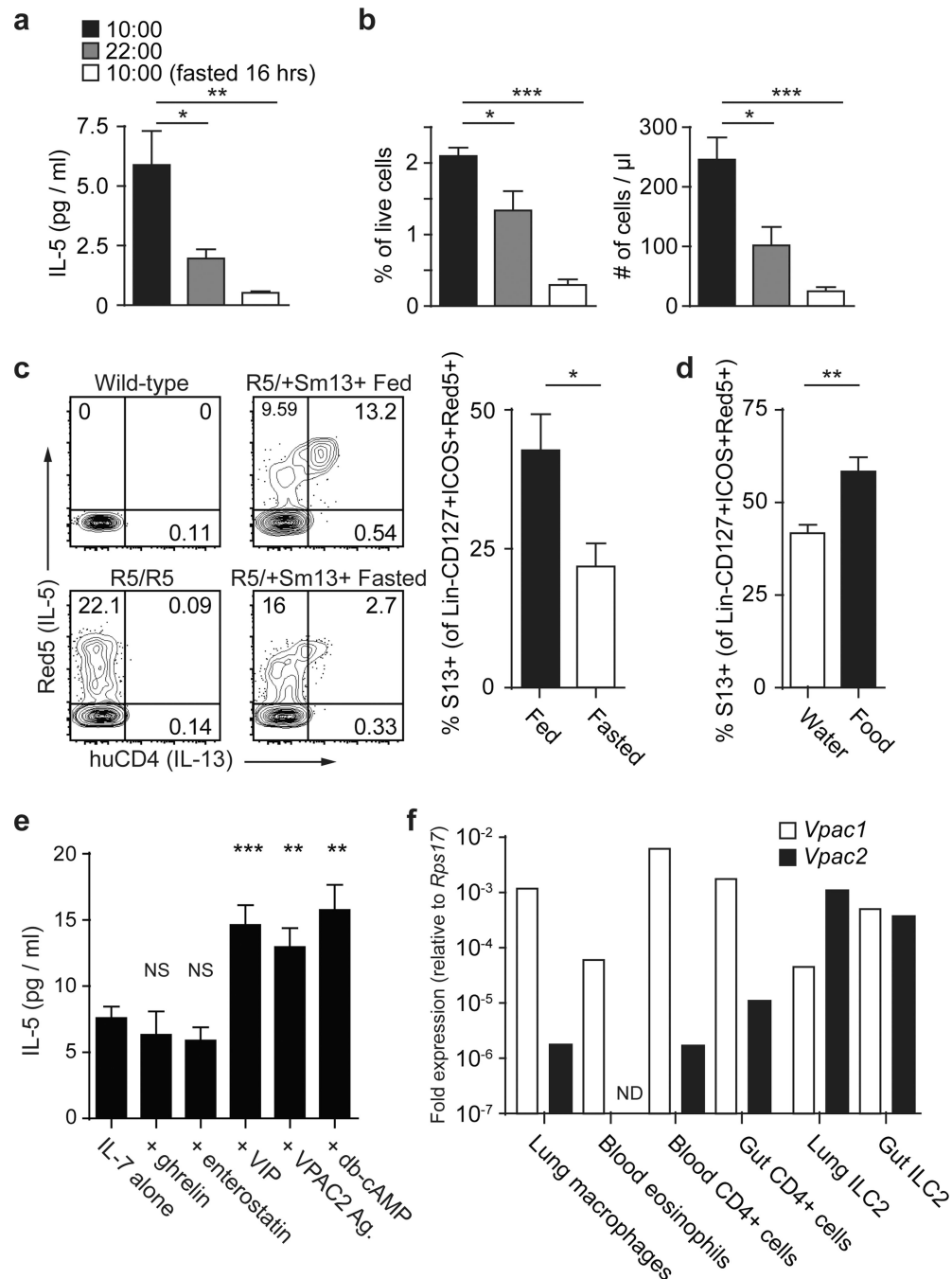


Figure 4. ILC2 respond to circadian and metabolic cues

a-b, Serum IL-5 and blood eosinophils at 10:00, 22:00 or at 10:00 after fasting. **c-d**, Flow cytometry of small intestine ILC2 (Lin-CD127+ICOS+) and percent of R5-hi ILC2 expressing S13 at 8:00 in mice on nighttime (black) or daytime (white) feeding (**c**) or in fasted mice given food (black) or water (white) by oral gavage (**d**). **e**, Supernatant IL-5 from intestinal Lin-CD45+KLRG1+ ILC2 cultured in IL-7 alone or with indicated reagents. **f**, Expression of *Vpac1* and *Vpac2* in sorted cells, relative to *Rps17*. Data pooled from independent experiments for 19 (AM), 6 (PM), or 5 (fasted) mice per group (**a**); 7 (AM), 4

(PM), or 8 (fasted) mice per group (**b**); 8 mice per group (**c**); 6 mice per group (**d**); or pooled averages of duplicate cultures from 6 (IL-7 alone, + VIP, + VPAC2 agonist) or 3 (all others) cell sorts from independent mice (**e**), or representative of two experiments of independent cell sorts (**f**). Represented as mean \pm SEM. Lin, Lineage markers (B220, CD11b, CD11c, Ly6G, Fc ϵ RI, and NK1.1); Rps17, 40S ribosomal protein S17; NS, not significant; *, $p < 0.05$; **, $p < 0.01$; ***, $p < 0.001$ by Student's t test.